

# Temporal-frequency tuning of cross-orientation suppression in the cat striate cortex

JOHN D. ALLISON, KEVIN R. SMITH, AND A.B. BONDS

Department of Electrical Engineering and Computer Science, Vanderbilt University,  
Nashville, Tennessee

(RECEIVED April 6, 2001; ACCEPTED October 23, 2001)

## Abstract

A sinusoidal *mask* grating oriented orthogonally to and superimposed onto an optimally oriented *base* grating reduces a cortical neuron's response amplitude. The spatial selectivity of cross-orientation suppression (XOR) has been described, so for this paper we investigated the temporal properties of XOR. We recorded from single striate cortical neurons ( $n = 72$ ) in anesthetized and paralyzed cats. After quantifying the spatial and temporal characteristics of each cell's excitatory response to a base grating, we measured the temporal-frequency tuning of XOR by systematically varying the temporal frequency of a mask grating placed at a *null* orientation outside of the cell's excitatory orientation domain. The average preferred temporal frequency of the excitatory response of the neurons in our sample was  $3.8 (\pm 1.5 \text{ S.D.})$  Hz. The average cutoff frequency for the sample was  $16.3 (\pm 1.7)$  Hz. The average preferred temporal frequency ( $7.0 \pm 2.6$  Hz) and cutoff frequency ( $20.4 \pm 6.9$  Hz) of the XOR were significantly higher. The differences averaged  $1.1 (\pm 0.6)$  octaves for the peaks and  $0.3 (\pm 0.4)$  octaves for the cutoffs. The XOR mechanism's preference for high temporal frequencies suggests a possible extrastriate origin for the effect and could help explain the low-pass temporal-frequency response profile displayed by most striate cortical neurons.

**Keywords:** Intracortical inhibition, Orientation tuning, Area 17, Nonlinearity

## Introduction

Hubel and Wiesel's original model of the orientation selectivity exhibited by striate cortical neurons is based on a linear summation of excitatory feedforward inputs from the lateral geniculate nucleus (Hubel & Wiesel, 1962). Subsequent studies (Reid & Alonso, 1995; Ferster et al., 1996) support their proposition. A strictly linear model of orientation selectivity is incompatible however with empirical evidence that a *mask* stimulus (e.g. a bar or grating) oriented orthogonally to and superimposed onto an optimally oriented excitatory *base* stimulus suppresses a cortical neuron's response to that base stimulus (Morrone et al., 1982; Bonds, 1989; DeAngelis et al., 1992). This nonlinear phenomenon is referred to as cross-orientation suppression (XOR), but this is in many cases a misnomer because the strongest suppression is often not induced by a mask stimulus oriented orthogonally to a neuron's preferred stimulus. Rather, it may be generated by a mask stimulus at a *null* (i.e. nonexcitatory) orientation near the edge of a cortical neuron's excitatory orientation-tuning domain where its response approaches maintained discharge levels (Bonds, 1989; Ringach et al., 1997). Similarly, Bauman and Bonds (1991) report that in the spatial-frequency domain, the strongest suppression occurs in most

cells when the spatial frequency of the mask is near the edge of excitatory spatial-frequency response domain.

The orientation (Bonds, 1989) and spatial-frequency (Bauman & Bonds, 1991) selectivity displayed by XOR suggests that it is cortical in origin. To understand fully XOR, however, we need a description of its temporal-response properties. Substantial differences in temporal processing are evident at different levels of the central visual pathways, so such data might also provide insight about its site of origin. We describe in this paper how the magnitude of XOR varies as a function of the temporal frequency of a mask stimulus. Our data demonstrate that the peak and cutoff frequencies displayed by XOR are significantly higher than the typical peak and cutoff frequencies exhibited by the excitatory response of most area 17 neurons. We conclude from these findings that XOR originates from a population of cortical inhibitory interneurons that prefer high temporal frequencies. Their temporal-response profile raises interesting questions about the source of their input and could help explain the low-pass shape of the temporal-frequency response functions exhibited by most striate cortical neurons.

## Methods

### *Surgical preparation*

We prepared 13 adult cats for single-unit recording from striate cortex following guidelines established by the American Physio-

Address correspondence and reprint requests to: A.B. Bonds, Department of Electrical Engineering and Computer Science, P.O. Box 1824, Station B, Vanderbilt University, Nashville, TN 37235, USA. E-mail: ab@vuse.vanderbilt.edu

logical Society and the Vanderbilt University Animal Care and Use Committee. One hour prior to surgery, each cat received intramuscular injections of acepromazine maleate and atropine sulfate (0.5 ml each). Anesthesia was induced with 5% Fluothane (halothane) in O<sub>2</sub>, a forelimb vein was cannulated and gas anesthesia was discontinued while subsequent anesthesia was maintained with Propofol delivered at a rate of at least 20.0 mg/kg/h as required for the remainder of surgery. A forelimb or hindlimb vein was cannulated for later infusion with paralytic agents. A tracheal cannula was inserted and the cat was mounted in a stereotaxic device. The scalp was reflected along the midline and electrodes were inserted over the lateral suprasylvian gyri for the monitoring of electroencephalogram (EEG). A 1 mm × 3 mm hole was drilled at Horsley-Clarke coordinates P4-L2, directly over the *area centralis* representation in area 17. (For one cat, the hole was placed at Horsley-Clarke coordinates P4-L5 in order to record from area 18 neurons.) The dura was incised, the electrode was positioned over an area free of surface vessels, and the hole was covered with agar mixed in lactated Ringers solution. Melted paraffin wax was poured over the agar to provide an effective hydraulic seal.

### Recording

The cats were initially paralyzed with 3 ml of Pavulon (pancuronium bromide; 2 mg/ml). Paralysis was maintained by infusion at a rate of 0.2 mg/kg/h. Lactated ringers solution was included in the infusate. Anesthesia was maintained with Propofol at 0.3 mg/kg/h and the cats were ventilated with a mixture of N<sub>2</sub>O:O<sub>2</sub>:CO<sub>2</sub> (75:23.5:1.5) at 30 strokes/min at a volume sufficient to hold expired pCO<sub>2</sub> at 3.9%. The animal's state of anesthesia and health were monitored *via* EEG and electrocardiogram (EKG). Rectal temperature was maintained at 37.5°C with a servo-controlled heat pad. Eyelids were retracted and the natural pupils were dilated by instillation of 10% phenylephrine HCL and 1% atropine sulfate in the conjunctival sacs. Contact lenses with 4-mm-diameter pupils were fitted to the nearest 0.5-m base curve radius and auxiliary lenses were added as dictated by direct ophthalmoscopy to render the retinae conjugate with the viewing screen 57 cm distant. Retinal landmarks (optic disk and *area centralis*) were projected onto the plotting screen with a reversible ophthalmoscope. All recorded cells had receptive fields located within 5 deg of the *area centralis*. Action potentials were recorded with glass-insulated tungsten microelectrodes (Levick, 1972) with tips 18–20 μm long and 2 μm wide at the shoulder.

### Stimulation, data acquisition, and processing

After hand-plotting the receptive field of a cell, we quantified its orientation selectivity, spatial-frequency selectivity, and temporal-frequency selectivity using computer-controlled presentations of sine-wave gratings at 28% contrast. A CRT display (Tektronix 608; mean luminance 110 cd/m<sup>2</sup>, P31 phosphor) with a 10-deg circular field was used as the primary stimulator. The display was compensated for linear modulation up to 75% contrast. Drifting sine-wave gratings were generated with a microprocessor-based pattern generator, similar in concept to that described by Milkman et al. (1978). The pattern generator supported independent control of the spatial frequency, phase, contrast, orientation, and drift rate of up to four patterns. Multiple patterns were superimposed by alternating frames of each pattern at a rate of 256/s; with two patterns, each pattern was presented at rate of 128/s. All stimulation was monocular.

The construction of 2-s, 128 bin/s poststimulus time histograms served as the primary data-analysis tool. For each set of measurements, the interleaved histogram technique of Henry et al. (1973) with randomization was used to reduce artifact from the inherent nonstationarity of visual cortex. Each experiment was constructed with measurements parametric on one variable (e.g. orientation or spatial frequency). A stimulus set was specified comprising each measuring condition as well as a null condition (uniform field at the mean luminance of the gratings) to assess the maintained discharge. Each element in the stimulus set was presented once, in random order with 1 s of mean luminance between each presentation, until the set was completed. Presentation of the set was then repeated in a different random order until each stimulus condition had been tested five times. With 4-s presentation periods, results are based on 20 s of averaging for each condition. The number of impulses per presentation was tracked to permit calculation of response variability.

After quantifying the "excitatory" spatiotemporal response profile of a neuron, we set the parameters of the base stimulus to the optimal values found during the tests described above. To measure the dependence of XOR on temporal frequency, a mask grating was superimposed onto the optimized base grating. The orientation of this mask was positioned at one null angle (see arrows in Fig. 1). (For 20 cells, a second set of experiments with the mask positioned at a second null orientation, on the "opposite side" of the tuning curve, was conducted. The goal was to stimulate separate populations of inhibitory neurons with different orientation selectivities and to compare the XOR temporal-frequency tuning functions produced by each.) The spatial frequency of the mask matched the base grating's spatial frequency. The contrast of each grating was adjusted so that the effective contrast of each was 28%. We varied the temporal frequency of the mask from 1 Hz to 20 Hz. Presentations of the base alone were randomly interleaved into the stimulus set in order to record the neuron's response to the optimized excitatory stimulus in the absence of the suppressive mask. This response represented the maximal response amplitude against which the XOR tuning functions were plotted (Bonds, 1989). We fit a Gaussian function to both sets of data to quantify both the excitatory and XOR temporal-frequency peaks and cut-offs for each neuron.

### Cell classification and response measurement

We first plotted receptive fields by hand and classified cells as simple or complex based on the criteria of Hubel and Wiesel (1962). We based final cell classification on responses to drifting sine-wave gratings by calculating each neuron's modulation index (Skottun et al., 1991). Cells with a modulation index greater than 1 were classified as simple and those with a modulation index less than 1 were classified as complex. This scheme means that the first harmonic response was used for simple cells while the DC response was used for complex cells. No differences were found between simple ( $n = 7$ ) and complex ( $n = 65$ ) cells, so we pooled the data from each group.

### Results

This laboratory and others have previously measured the spatial selectivity of XOR by varying the orientation (Morrone et al., 1982; Bonds, 1989; DeAngelis et al., 1992) and spatial frequency (Bauman & Bonds, 1991) of a mask grating that is superimposed onto an optimized excitatory base grating. To measure the temporal-

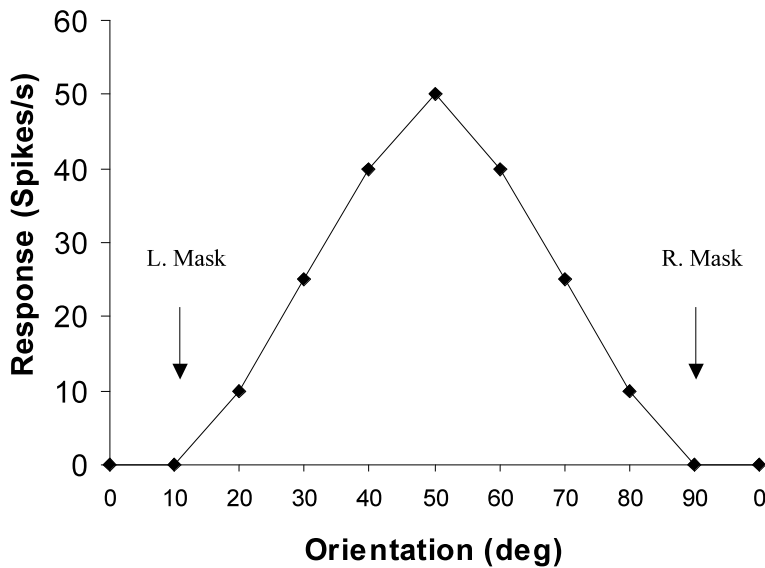


**Fig. 1.** Orientation tuning function of a striate cortical neuron. The response of a neuron is plotted as a function of stimulus orientation. The strongest suppression occurs at *null* orientations near each boundary of the excitatory tuning function (*arrows*). We used a stimulus orientation to the left (along the abscissa) of the peak for the *left mask* and an orientation to the right of the peak along the abscissa for the *right mask*.

frequency selectivity of XOR, we held constant the orientation and spatial frequency of the mask grating at values that produced strong suppression, but varied its temporal frequency. We recorded the effects of temporal variation of the mask on the response amplitude of 72 striate cortical neurons and found that the mask suppressed the response of all but eight neurons. For the 64 neurons that exhibited suppression, the magnitude of suppression depended on the temporal frequency of the mask.

#### Examples of excitatory and XOR temporal-frequency response functions

Figs. 2A–2D illustrate data recorded from four typical neurons in our sample. Each panel shows one neuron's excitatory response (*filled circles*) plotted as a function of the temporal frequency of the spatially optimized base stimulus. A Gaussian function fit to the data points using the method of least squares provided measurements of the temporal-frequency peak (*Exc Peak*) and cutoff frequency (*Exc Cutoff*) for each cell. [Although we had no *a priori* reason for choosing a Gaussian, this function provided a simple way to quantify the peak and cutoff frequency for each cell and we found the fits acceptable for this purpose. For example, the  $R^2$  of the excitatory functions shown in Figs. 2A–2D were 0.97, 0.94, 0.98, and 0.99, respectively. The  $R^2$  obtained from our sample of 72 neurons ranged from 0.62 to 0.99 and averaged 0.97 ( $\pm .05$ ).

The Gaussian function fit to the data points (*open circles*) recorded in the presence of the mask shows the temporal-frequency tuning of the XOR. [The  $R^2$  of the XOR tuning functions in Figs. 2A–2D are 0.69, 0.95, 0.94, and 0.99, respectively. The  $R^2$  of the XOR functions obtained from our sample of neurons ranged from 0.62 to 0.99 and averaged 0.82 ( $\pm 0.23$ )]. For these data points, zero on the ordinate axis represents the average response of the cell to stimulation with the base stimulus alone (i.e. the mask at 0% contrast) and the abscissa shows the temporal frequency of the mask. The response of each neuron was clearly suppressed by the presence of the mask because each data point lies below zero. Moreover, the magnitude of the suppression depended on the temporal frequency of the mask. In Fig. 2A, for example, zero represents a response amplitude of approximately

60 spikes/s. The maximal suppression (*XOR Peak*) occurred when the mask drifted at a rate of 7.4 Hz. This value is 1.0 octave higher than this cell's excitatory peak of 3.7 Hz. At this temporal frequency, the mask reduced the response of the neuron by nearly 40 spikes/s. The cutoff frequency of this cell's XOR response (*XOR Cutoff*) was 19.6 Hz for this cell, that is, 0.4 octaves higher than the cell's excitatory cutoff frequency of 15.5 Hz. Similar results are shown by the examples in panels 2B–2D.

#### Excitatory and XOR temporal-frequency peaks

The parameters of the excitatory and XOR temporal-frequency tuning functions recorded from most neurons in our sample support the evidence from our examples that XOR is tuned higher than the excitatory response of most area 17 neurons. The scatterplot in Fig. 3A, for example, shows the peak frequencies obtained from the XOR (ordinate) and excitatory (abscissa) tuning functions of each neuron in our sample. The majority of data points in this figure lie above the unity line. This pattern supports the contention that the suppressive neural mechanism being driven by the mask is tuned higher in the temporal-frequency domain than is the excitatory input to area 17 neurons. Fig. 3B shows the distribution of excitatory (*filled bars*) and XOR (*open bars*) peak temporal frequencies recorded from our sample of neurons. Most neurons displayed excitatory temporal frequency peaks between 2 and 6 Hz. One neuron displayed an excitatory peak frequency as high as 9 Hz. The average excitatory peak recorded from the sample was 3.8 ( $\pm 1.5$ ) Hz.

In contrast, most neurons displayed XOR temporal-frequency peaks between 6 and 8 Hz. Some cells even exhibited peaks higher than 10 Hz. The XOR tuning functions recorded from the sample displayed an average peak of 7.0 ( $\pm 2.6$ ) Hz. A *t*-test revealed that the XOR peaks recorded from our sample were significantly higher than the excitatory peaks ( $t = 11.2$ ;  $P < 0.001$ ). Notably, the distribution of XOR peaks recorded from our sample of area 17 neurons resembles the distribution of excitatory peaks we recorded from 24 neurons in area 18, which typically exhibit higher temporal-frequency peaks and cutoffs than area 17 neurons (Movshon et al., 1978). The average peak temporal frequency recorded from area

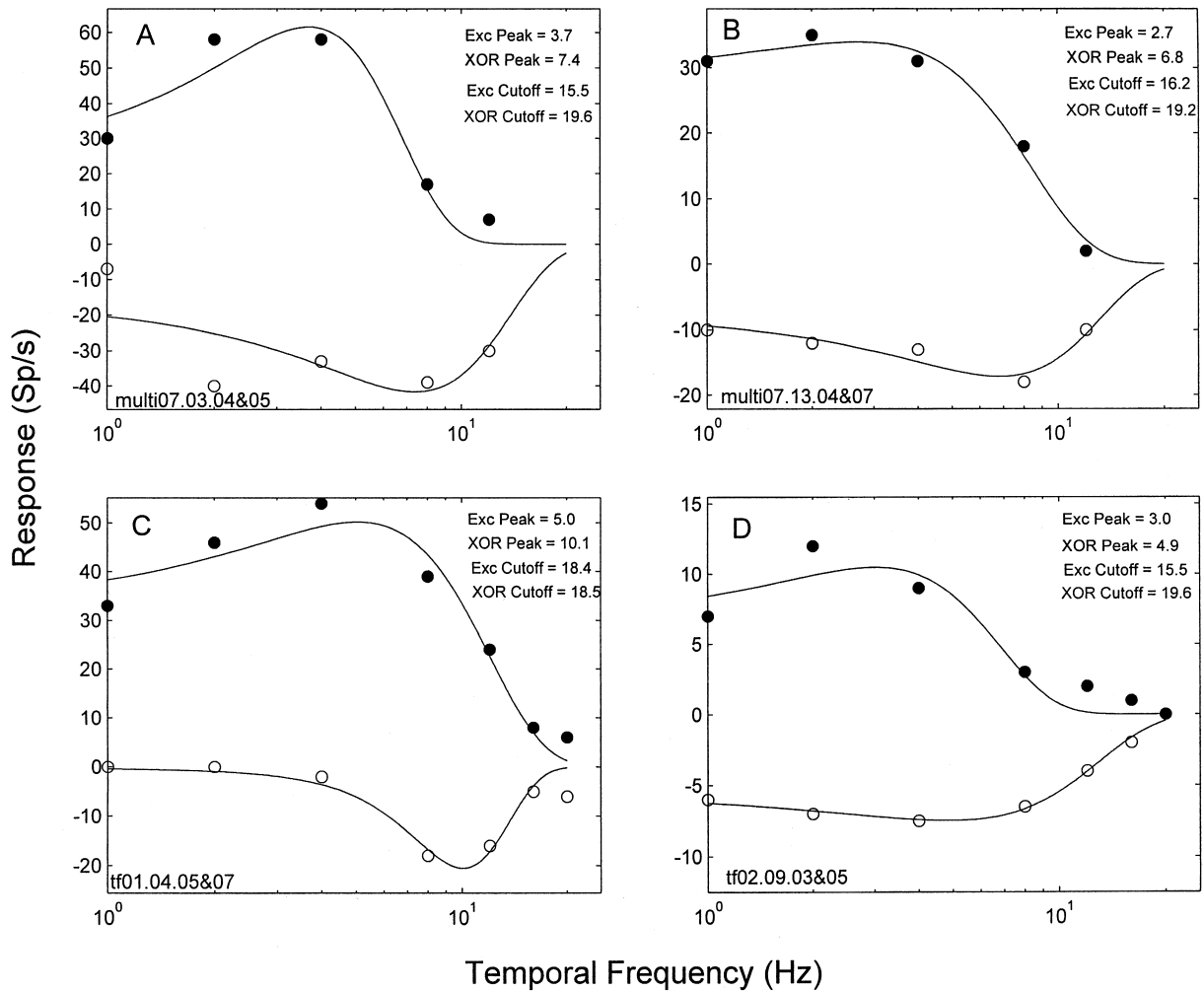


**Fig. 2.** Cross orientation suppression varies as a function of temporal frequency. The baseline response amplitude recorded from four neurons is plotted as a function of the temporal frequency of an optimized base grating (*solid circles*) and fitted with a Gaussian function. The response of the neurons when simultaneously stimulated with the base grating and a superimposed mask grating at the null orientation are also shown (*open circles*). For the XOR functions, zero represents the cell's averaged response with the mask at 0% effective contrast (i.e. the response to the spatiotemporally optimized base presented alone at 28% effective contrast). In the presence of a mask at 28% effective contrast, each neuron's response is suppressed (i.e. it falls below zero). The magnitude of suppression varies as a function of the temporal frequency of the mask. In most cases, the peak suppression occurred at a temporal frequency that was higher than the excitatory peak frequency. The excitatory peak (*Exc Peak*), XOR peak (*XOR Peak*), excitatory cutoff (*Exc Cutoff*), and XOR cutoff (*XOR cutoff*) are indicated. The cat number, cell number, and run number are also indicated (e.g. multi07.03.04&05).

18 neurons ( $7.2 \pm 3.1$  Hz) was indistinguishable from the XOR peak recorded from area 17.

We calculated the difference (in octaves) between the excitatory and XOR peak frequencies recorded from each neuron in our sample. The distribution of differences is plotted in Fig. 3C. For most neurons ( $n = 38$ ), the XOR peak was about one octave higher than the excitatory peak. The differences ranged from  $-0.97$  (i.e. the excitatory peak was higher,  $n = 7$ ) to 2.29 octaves. When averaged across the sample of cells, the XOR peak frequency was  $1.1 (\pm 0.6)$  octaves higher than the excitatory peak.

We recorded XOR temporal-frequency tuning functions from 20 neurons using two different null orientations (one on each side of the excitatory peak). (We refer to these stimulus orientations as "left" or "right" depending on where they lie along the abscissa of an orientation-tuning function relative to the preferred stimulus

orientation, cf. Fig. 1.) For 17 of these cells, we were able to fit a Gaussian to both XOR functions and compare the parameters. The purpose of this experiment was to stimulate two different populations of inhibitory neurons with dissimilar orientation preferences, to determine whether they provide similar amounts of XOR to a recorded neuron. We hoped to determine whether, for a given neuron, the XOR mechanism was "symmetrical" around the excitatory temporal-frequency peak. The scatterplot in Fig. 3D illustrates the peaks produced by the left (abscissa) and right (ordinate) null orientations for each of the 17 neurons tested in this manner. If the two mask positions produced identical inhibitory temporal-frequency peaks, all the points should lie on the unity line. The results of this test are not conclusive. Some of the data points fall away from the line, indicating that the peak XOR frequency observed depended on the angle of the mask. For these cells,

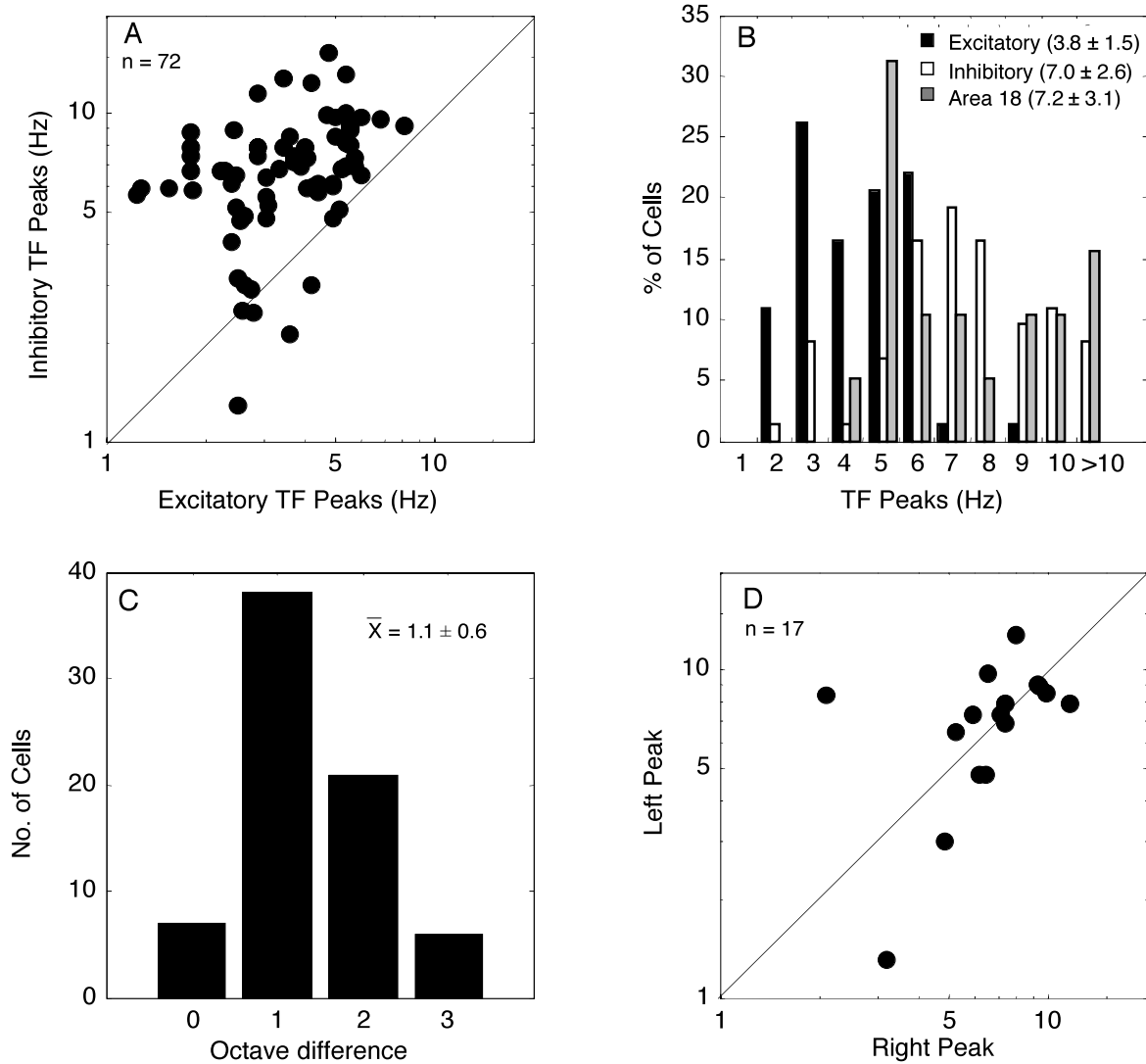


**Fig. 3.** Comparison of excitatory and XOR peak temporal frequencies. (A) The scatterplot shows the excitatory (abscissa) and XOR (ordinate) peak temporal frequencies recorded from each neuron in our sample ( $n = 72$ ). The XOR peaks recorded from most neurons were higher than their excitatory peaks. (B) The distributions of excitatory (*dark bars*) and XOR (*open bars*) peak temporal frequencies show that most of the neurons had an excitatory peak temporal frequency between 2 and 6 Hz. Only one neuron (visible in A) had an excitatory peak temporal frequency above 8 Hz. The excitatory peak recorded from the sample averaged  $3.8 (\pm 1.5)$  Hz. In contrast, roughly half of the neurons in our sample had XOR peak temporal frequencies between 6 and 8 Hz and about 10% had peaks above 10 Hz. On average, the XOR peak frequency recorded from the sample was  $7.0 (\pm 2.6)$  Hz. Interestingly, the distribution of inhibitory peaks resembled the distribution of peak temporal frequencies recorded from the excitatory responses of a small sample ( $n = 24$ ) of area 18 cells (*gray bars*), which averaged  $7.2 (\pm 3.1)$  Hz. (C) For most neurons, the XOR peak was about one octave higher than the excitatory peak. For some neurons, however, the XOR peak was two or three octaves higher than the excitatory peak. The XOR peak temporal frequency was, on average,  $1.1 (\pm 0.6)$  octaves higher than the excitatory peak temporal frequency. (D) For 17 neurons, we measured and compared the XOR peak temporal frequencies produced by the mask at two different *null* orientations. The scatterplot illustrates the mixed results. For some cells, the two null orientations produced different peaks while, for other cells, the peaks were indistinguishable.

therefore, the neural substrate of XOR appears to be asymmetrical. Other cells fall close to the unity line, indicating that the peak XOR frequency did not depend on the mask orientation. For these cells, the neural substrate of XOR appears to be symmetrical.

*Excitatory and XOR temporal-frequency resolution*

We measured the temporal-frequency resolution (i.e. cutoff frequency) of the excitatory and XOR responses of each neuron in

our sample. Fig. 4A shows each neuron’s excitatory (abscissa) and XOR (ordinate) temporal frequency. As was the case with the peak temporal frequencies (Fig. 3A), most data points fall above the unity line. This pattern demonstrates that the cutoff frequency of the XOR recorded from most neurons was higher than their excitatory cutoff frequency. The histograms in Fig. 4B show the distributions of the excitatory (*black bars*) and XOR (*open bars*) temporal-frequency cutoffs recorded from the sample. The excitatory cutoff frequency for most neurons occurred between 15 and

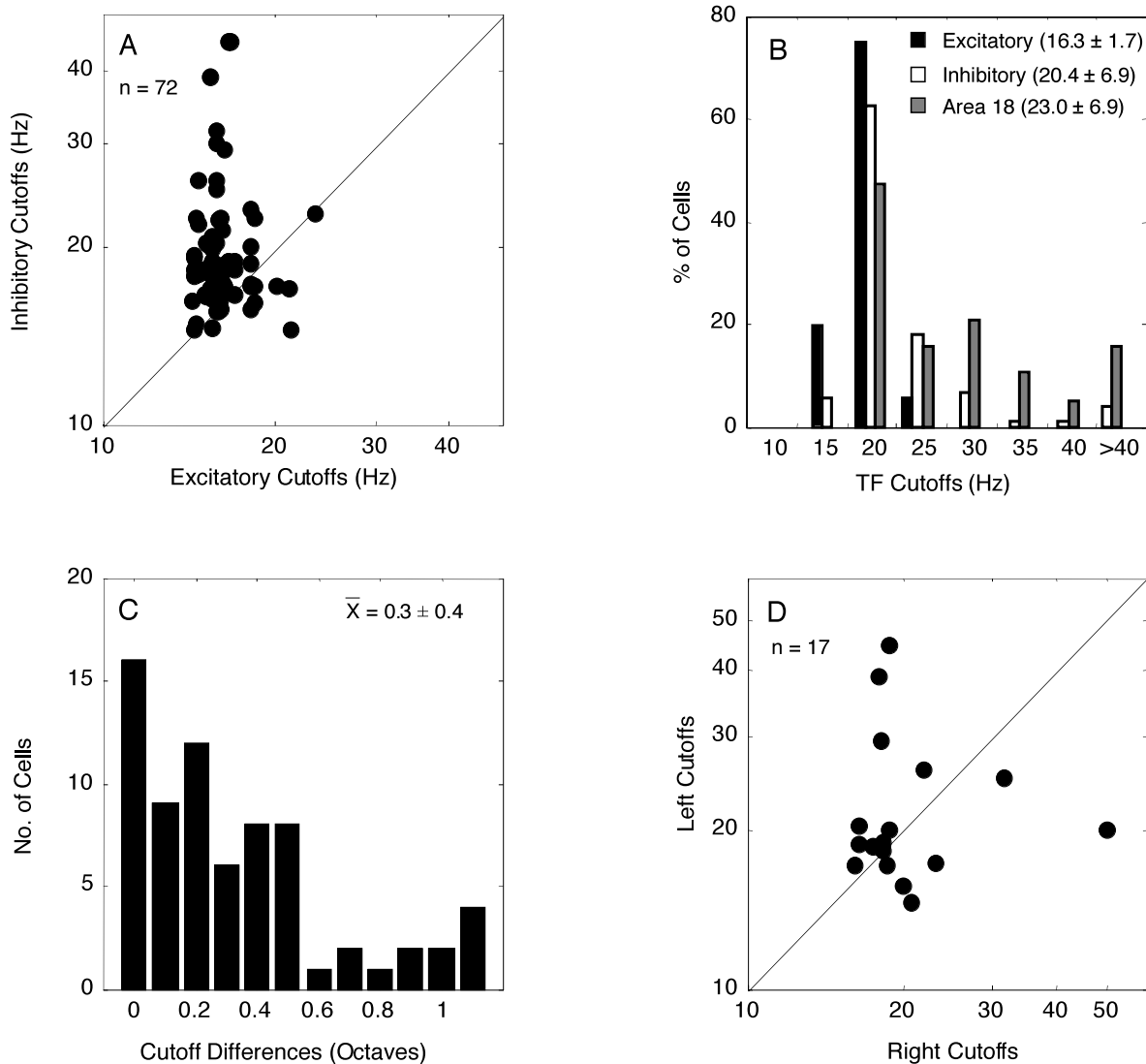


**Fig. 4.** Comparison of excitatory and XOR temporal frequency cutoffs. (A) The scatterplot shows the excitatory (abscissa) and XOR (ordinate) temporal-frequency cutoffs recorded from our sample of neurons. The XOR cutoffs recorded from most neurons were higher than the excitatory cutoffs. (B) The distributions of excitatory (dark bars) and XOR (open bars) temporal-frequency cutoffs show that most neurons had an excitatory temporal-frequency cutoffs between 15 and 20 Hz (mean =  $16.3 \pm 1.7$  Hz). Most of the sample had XOR cutoff frequencies between 20 and 25 Hz (mean =  $20.4 \pm 6.9$  Hz). The XOR pattern resembled the pattern recorded from the excitatory responses of a small sample of area 18 cells (gray bars, mean =  $23.0 \pm 6.9$  Hz). (C) For most neurons, the XOR cutoff frequency was one octave higher than the excitatory cutoff frequency. On average, the XOR cutoff frequency was  $0.3 (\pm 0.4)$  octaves higher than the excitatory cutoff frequency. (D) We measured and compared the XOR peak temporal frequencies produced by the mask at two different orientations. For some neurons tested, the temporal-frequency cutoff produced when the mask was tilted counterclockwise relative to the base (i.e. to the left, *abscissa*) was not identical to the inhibitory peak found when the mask was tilted clockwise (ordinate). For others, the cutoffs were the same, regardless of mask orientation.

20 Hz (see Fig. 4A). The average excitatory cutoff frequency recorded from the sample was  $16.3 (\pm 1.7)$  Hz. The distribution of XOR cutoffs exhibits a peak near 20 Hz. The average suppressive temporal frequency cutoff was  $20.4 (\pm 6.9)$  Hz. The temporal resolution of XOR was significantly higher than the excitatory resolution ( $t = 4.9$ ;  $P < 0.001$ ). Like the temporal-frequency peaks, the distribution of XOR cutoff frequencies was similar to the distribution recorded from area 18 neurons (shaded bars). This distribution also peaked near 20 Hz, with an average cutoff frequency of  $23.0 (\pm 6.9)$  Hz.

We calculated the difference (in octaves) between the excitatory and XOR cutoff frequencies for each neuron in our sample.

The distribution of differences between the cutoff frequencies is shown in Fig. 4C. Most neurons displayed an XOR cutoff frequency that was between 0.1 and 0.5 octaves higher than the excitatory cutoff frequency. On average, the XOR cutoff frequency recorded from our sample of cells was  $0.3 (\pm 0.4)$  octaves higher than the excitatory cutoff frequency.

For the 17 neurons that were tested with separate presentations of the mask at two different null orientations, we compared the XOR cutoff frequencies produced during each measurement series (Fig. 4D). For some neurons in this small sample, the data points recorded when the mask was oriented counterclockwise from the preferred axis (abscissa) did not match the points recorded when

the mask angle was clockwise from the excitatory stimulus (ordinate). For others, the cutoff frequencies did match. Thus, we found no systematic pattern of one mask producing a higher cutoff frequency than the other.

### Discussion

A mask stimulus superimposed onto an excitatory base stimulus, but oriented outside the excitatory domain range of a cortical neuron, suppresses the neuron's response to the base stimulus. The magnitude of suppression is orientation (Bonds, 1989) and spatial frequency (Bauman & Bonds, 1991) dependent, indicating that the neural mechanism responsible for XOR is spatially selective. The current results show that the neural substrate of XOR also exhibits some degree of temporal-frequency selectivity. The most interesting finding is that XOR is tuned to temporal frequencies higher than the peak temporal frequencies found in the excitatory response of most area 17 neurons. Furthermore, XOR exhibits a higher temporal resolution (i.e. cutoff frequency) than most area 17 cells. Together, these results suggest that the neural substrate of XOR is a population of inhibitory interneurons selective for high temporal frequencies. This population of neurons might also help convert the broad temporal-frequency tuning from the lateral geniculate nucleus (LGN) into the low-pass response observed in most striate cortical neurons.

#### *XOR, intracortical inhibition, and orientation selectivity*

The orientation (Bonds, 1989) and spatial-frequency (Bauman & Bonds, 1991) selectivity exhibited by XOR is consistent with the notion that an inhibitory mechanism within striate cortex itself forms the neural substrate for XOR. Despite empirical evidence to the contrary (Reid & Alonso, 1995; Ferster et al., 1996), a functional role for intracortical inhibition should not be surprising given that approximately 20% of striate cortical neurons are GABAergic (Gabbott & Somogyi, 1986; Hendry et al., 1987). GABAergic inhibition sharpens orientation selectivity (Sillito, 1975; Pflieger & Bonds, 1995) and could be a source of the XOR observed in masking experiments. There is no empirical evidence, however, to support the hypothesis that GABAergic neurons within area 17 are the direct source of XOR. In fact, the high temporal-frequency selectivity exhibited by the XOR recorded from our sample of neurons is suggestive of an external influence because we rarely record from area 17 neurons with such selectivity.

#### *Intracortical feedback: A drive for suppression?*

We found indirect evidence that supports the possibility that the neural mechanism of XOR originates from outside of area 17. The average peaks and cutoffs of the neural substrate of XOR closely resemble the data we recorded from the small sample of area 18 neurons, which were consistent with prior studies (e.g. Movshon et al., 1978). Feedback from area 18 could therefore be a source of the drive for the temporal-frequency-dependent suppression we recorded in area 17. In fact, experiments show that when cells in layer V (Alonso et al., 1993) or layers 2/3 (Martinez-Conde et al., 1999) of area 18 are reversibly inactivated by injections of GABA, the response of area 17 neurons to high-velocity stimuli is enhanced.

There is some anatomical evidence that area 18 could induce XOR in area 17 *via* a feedback path responsive to high temporal frequencies. LGN Y-cells predominantly project to area 18 while

X-cells innervate area 17 (Gilbert & Kelly, 1975; Levay & Ferster, 1977) and Y-cells are more sensitive to high temporal frequencies than X-cells (Lehmkuhle et al., 1980). However, feedback to area 17 from area 18 is thought to be exclusively excitatory (Gilbert & Kelly, 1975), so the presence of such feedback does not fully explain the presence of XOR nor the suppression of responses to high frequencies exhibited by most area 17 neurons. Some intermediate inhibitory connections would need to exist, and these would most likely be located within area 17.

In our laboratory, we rarely encounter striate cortical neurons that exhibit the temporal-frequency response profiles (e.g. peak frequencies above 8 Hz or so) that would be necessary to explain the presence of high-frequency-sensitive XOR, originating either within or outside area 17. There is some evidence that such neurons exist, however. Orban et al. (1981) have found area 17 neurons that respond to velocities near 100 deg/s. This would suggest the presence of area 17 neurons with temporal-frequency cutoffs in the range of 50 Hz, a figure well within the range necessary to explain the presence of a high-frequency-sensitive XOR mechanism. If such neurons proved to be inhibitory interneurons, they could be the source of the high-frequency-sensitive XOR we found in the current study.

#### *Intracortical suppression of high-frequency input from LGN*

The temporal-frequency response profile exhibited by XOR in the present study suggests a high-frequency-selective inhibitory neural substrate might also influence the temporal-frequency tuning of area 17 neurons. The temporal-frequency curves recorded from most striate cortical neurons in cats reveal low-pass profiles with peaks between 2–4 Hz and cutoffs around 15 Hz (Ikeda & Wright, 1975; Movshon et al., 1978). These characteristics contrast those found in the response patterns of LGN neurons (Lehmkuhle et al., 1980; Saul & Humphrey, 1990; Hamamoto et al., 1994; Mukherjee & Kaplan, 1995). While the peak temporal frequency exhibited by most LGN neurons is similar to that typically found in striate cortex, the temporal resolution (i.e. cutoff frequency) of most LGN neurons is generally higher than the resolution observed in area 17 neurons (Lehmkuhle et al., 1980; Saul & Humphrey, 1990). Lehmkuhle et al. (1980) found that, on average, the cutoff frequency of LGN Y-cells is near 30 Hz while that of X-cells is just above 20 Hz. Although Saul and Humphrey (1990) found no statistical differences in the cutoff frequencies between these two populations of LGN cells, they do report that nonlagged cells exhibit significantly higher cutoff frequencies than lagged cells. On average, the resolution of lagged LGN cells is just under 20 Hz and ranges as high as 30 Hz. Nonlagged cells' average temporal resolution is close to 30 Hz and ranges as high as 60 Hz. The average temporal resolution of Y-cells (Lehmkuhle et al., 1990) or nonlagged cells (Saul & Humphrey, 1994) is consistent with behavioral evidence that the temporal resolution of cats is around 30 Hz (Blake & Camisa, 1977). Our data indicate the existence of an inhibitory neural mechanism tuned substantially higher in the temporal-frequency domain than most area 17 neurons. Although it is not immediately evident how the temporal-frequency response profile of XOR could affect area 17 neurons occurs during stimulation with one grating at the optimal orientation, the XOR tuning properties point to the existence of an inhibitory substrate [that could include neurons with similar orientation preferences of a recorded neuron (Ferster et al., 1996)] that could suppress a cortical cell's responses to high temporal-frequency stimuli. The

temporal-frequency response profile of excitatory and inhibitory synapses would need to be compared to directly address this issue.

### Acknowledgments

We thank Jason Samonds, Mollie Atherton, and Heather Crouch for their assistance with data collection and analysis during this study. The work was supported by National Eye Institute Grant No. EY03778.

### References

- ALONSO, J.M., CUDEIRO, J., PEREZ, R., GONZALEZ, F. & ACUNA, C. (1993). Influence of layer V area 18 of the cat visual cortex on responses of cells in layer V of area 17 to stimuli of high velocity. *Experimental Brain Research* **93**, 363–366.
- BAUMAN, L.A. & BONDS, A.B. (1991). Inhibitory refinement of spatial frequency selectivity in single cells of the cat striate cortex. *Vision Research* **31**, 933–944.
- BLAKE, R. & CAMISA, J.M. (1977). Temporal aspects of spatial vision in the cat. *Experimental Brain Research* **28**, 325–333.
- BONDS, A.B. (1989). Role of inhibition in the specification of orientation selectivity of cells in the cat striate cortex. *Visual Neuroscience* **2**, 41–55.
- DEANGELIS, G.C., ROBSON, J.G., OHZAWA, I. & FREEMAN R.D. (1992). Organization of suppression in receptive fields of neurons in cat visual cortex. *Journal of Neurophysiology* **68**, 144–163.
- FERSTER, D., CHUNG, S. & WHEAT, H. (1996). Orientation selectivity of thalamic input to simple cells of cat visual cortex. *Nature* **380**, 249–252.
- GABBOTT, P.L.A. & SOMOGYI, P. (1986). Quantitative distribution of GABA-immunoreactive neurons in the visual cortex (area 17) of the cat. *Experimental Brain Research* **61**, 323–331.
- GILBERT, C.D. & KELLY, J.P. (1975). The projections of cells in different layers of the cat's visual cortex. *Journal of Comparative Neurology* **163**, 81–106.
- HAMAMOTO, J., CHENG, H., YOSHIDA, K., SMITH, E.L. & CHINO, Y.M. (1994). Transfer characteristics of lateral geniculate nucleus X-neurons in the cat: Effects of temporal frequency. *Experimental Brain Research* **98**, 191–199.
- HENDRY, S.H.C., SCHWARK, H.D., JONES, E.G. & YAN, J. (1987). Numbers and proportions of GABA-immunoreactive neurons in different areas of monkey visual cortex. *Journal of Neuroscience* **7**, 1503–1519.
- HENRY, G.H., BISHOP, P.O., TUPPER, R.M. & DREHER, B. (1973). Orientation specificity of cells in cat striate cortex. *Vision Research* **13**, 1771–1779.
- HUBEL, D.H. & WIESEL, T. N. (1962). Receptive fields, binocular interaction, and functional architecture in the cat's visual cortex. *Journal of Physiology* **160**, 106–154.
- IKEDA, H. & WRIGHT, M.J. (1975). Spatial and temporal properties of 'sustained' and 'transient' neurons in area 17 of the cat's visual cortex. *Experimental Brain Research* **22**, 363–383.
- LEHMKUHLE, S., KRATZ, K.E., MANGEL, S.C. & SHERMAN, S.M. (1980). Spatial and temporal sensitivity of X- and Y-cells in dorsal lateral geniculate nucleus of the cat. *Journal of Neurophysiology* **43**, 520–541.
- LEVAY, S. & FERSTER, D. (1977). Relay classes in the lateral geniculate nucleus of the cat and the effects of visual deprivation. *Journal of Comparative Neurology* **172**, 563–584.
- LEVICK, W.R. (1972). Another tungsten microelectrode. *Medical and Biological Engineering* **10**, 510–515.
- MARTINEZ-CONDE, S., CUDEIRO, J., GRIEVE, K.L., RODRIGUEZ, R., RIVADULLA, C. & ACUNA, C. (1999). Effects of feedback projections from area 18 layers 2/3 to area 17 layers 2/3 in the cat visual cortex. *Journal of Neurophysiology* **82**, 2667–2675.
- MILKMAN, N., SHAPLEY, R.M. & SCHICK, G. (1978). A microcomputer-based visual stimulator. *Behavior Research Methods and Instrumentation* **10**, 539–545.
- MORRONE, M.C., BURR, D.C. & MAFFEI, L. (1982). Functional implications of cross-orientation inhibition of cortical visual cells. *Proceedings of the Royal Society B (London)* **216**, 335–354.
- MOVSHON, J.A., THOMPSON, I.D. & TOLHURST, D.J. (1978). Spatial and temporal contrast sensitivity of neurons in area 17 and 18 of the cat's visual cortex. *Journal of Physiology* **283**, 101–120.
- MUKHERJEE, P. & KAPLAN, E. (1995). Dynamics of neurons in the cat lateral geniculate nucleus: *In vivo* electrophysiology and computational modeling. *Journal of Neurophysiology* **74**, 1222–43.
- ORBAN, G.A., KENNEDY, H. & MAES, H. (1981). Response to movement of neurons in area 17 and 18 of the cat: Velocity sensitivity. *Journal of Neurophysiology* **45**, 1043–1058.
- PFLEGER, B. & BONDS, A.B. (1995). Dynamic differentiation of GABA<sub>A</sub>-sensitive influences on orientation selectivity of complex cells in the cat striate cortex. *Experimental Brain Research* **104**, 81–88.
- REID, R.C. & ALONSO, J.M. (1995). Specificity of monosynaptic connections from thalamus to visual cortex. *Nature* **378**, 281–284.
- RINGACH, D.L., HAWKEN, M.J. & SHAPLEY, R. (1997). Dynamics of orientation tuning in macaque primary visual cortex. *Nature* **387**, 281–284.
- SAUL, A.B. & HUMPHREY, A.L. (1990). Spatial and temporal response properties of lagged and nonlagged cells in cat lateral geniculate nucleus. *Journal of Neurophysiology* **64**, 206–224.
- SILLITO, A.M. (1975). The contribution of inhibitory mechanisms to the receptive-field properties of neurons in the striate cortex of the cat. *Journal of Physiology* **250**, 305–329.
- SKOTTUN, B.C., DEVALOIS, R.L., GROSOFF, D.H., MOVSHON, J.A., ALBRECHT, D.B. & BONDS, A.B. (1991). On classifying simple and complex cells according to response modulation. *Vision Research* **31**, 1079–1088.